International Journal of Technology (2016) 2: 264-273
ISSN 2086-9614 © IJTech 2016

OPTIMIZATION OF HYDROGEN STORAGE CAPACITY BY PHYSICAL ADSORPTION ON OPEN-ENDED SINGLE-WALLED CARBON NANOTUBE AS DIAMETER FUNCTION

Nasruddin[1*], Engkos A. Kosasih[1], Budhi Kurniawan[2], Supriyadi[1], I.A. Zulkarnain[3]

[1] *Department of Mechanical Engineering, Faculty of Engineering, Universitas Indonesia, Kampus UI Depok, Depok 16424, Indonesia*
[2]*Department of Physics, Faculty of Mathematics and Natural Sciences, Universitas Indonesia, Kampus UI Depok, Depok 16424, Indonesia*
[3] *Department of Mechanical Engineering, Faculty of Engineering, President University, Cikarang 17550, Indonesia*

(Received: October 2015 / Revised: December 2015 / Accepted: January 2016)

ABSTRACT

In this paper, we perform combination methods of semi-empirical research, a theoretical approach, and force-matching to determine the optimum adsorption capacity on an open-ended single-walled carbon nanotube (SWCNT) as a diameter function. Using a semi-empirical study, we can determine the value of monolayer coverage and isosteric heat of adsorption from available thermodynamic data. By completing the semi-empirical study, we carried out quantum mechanical calculations to determine the adsorption energy on the interior and exterior of SWCNTs. Furthermore, monolayer coverage, specific surface area, and maximum adsorption capacity as the main quantity in the adsorption process was estimated using the combination method of force-matching and a classical Lennard-Jones potential model. Hydrogen physisorption was investigated on zig-zag SWCNTs at conditions for a pressure range of 0.1 to 10 MPa at 233 K and 298.15 K temperature. The adsorption of all data can be explained with the Toth model. The results shows the SWCNT exterior physisorption energy range between 1.35 to 1.62 kcal/mol. The interior range from 1.22 to 2.43 kcal/mol. With a wide degree of temperature and pressure variations, we obtained an optimum SWCNT diameter of 8-12 Å . At the optimum diameter maximum adsorption capacity, we achieved 1.75 wt% at 233 K and an operating pressure of 10 MPa.

Keywords: Adsorption energy; Hydrogen; Isotropic; Monolayer coverage; SWCNT

1. INTRODUCTION

Hydrogen has attracted attention in recent decades due to the success of the "Hydrogen Economy"; it is renewable, highly efficient, sustainable, clean, and lightweight (Gayathri et al., 2010). Its thermal efficiency is higher compared to fossil based energy, and it is more environmentally friendly. The supply of hydrogen is sustainable, and it can easily be produced from others substances that contain hydrogen. These advantages have made hydrogen the most promising energy source of the future (Satyapal et al., 2007).

Storage is the main obstacle keeping hydrogen from being massively applied. Recently, the US Department of Energy (DoE) determined that before 2017, hydrogen storage gravimetrically

---

*Corresponding author's email: nasruddin@eng.ui.ac.id, Tel. +62-21- 7270032, Fax. +62-21- 7270033
Permalink/DOI: http://dx.doi.org/10.14716/ijtech.v7i2.2987

should achieve 5.5 wt% with a volumetric density of 40 kg/m^3 on 233 to 353 K and an operation pressure of 10 MPa. To meet this target, extensive research was conducted to find optimum ways to store hydrogen (Chen & Huang, 2008). Nowadays, compressed hydrogen (Zheng et al., 2012) or liquefaction are the most common ways to store hydrogen. Both are expensive, unsafe, volumetrically inefficient, and have high losses due to evaporation (Zhou, 2005). Metal hydride has high storage capacity, but production costs are expensive—and it needs a high temperature to relase the hydrogen. Hydrogen can also be stored chemically bonded in covalent and ionic compounds, but technically, both methods have serious drawbacks (Hamilton et al., 2009).

These problems can be solved if same amount of hydrogen can be stored in lower pressure at ambient temperature. This can be done by adding adsorbent material to the storage tanks. In recent years, hydrogen storage materials are focused to metal hydrides (Luo et al., 2007), chemical hydrides (Biniwale et al., 2008), and physisorption-based storage. Carbon-based nano structured holds play an importamt role in these processes (Barghi et al., 2014). Among the various hydrogen storage options, only storage in solid state materials seems promising (Sankaran & Viswanathan, 2007) due to reversibility, fast kinetics, and high capacities (Qiu et al., 2014). Among these, a carbon nanotube (CNT) has a number of favorable values, such as a porous nature, high surface area, vacancy space, high stability, and the fact that it is lightweight (Knippenberg et al., 2008).

The existence of adsorbent material may attract hydrogen gas molecules to its surface. Many researchers have searched for the best adsorbent material to store hydrogen gas molecules. CNT is one promising candidate. Its capability to store hydrogen was first investigated by Dillon et al. (1997). They stated that CNTs can store hydrogen gas up to 10 wt% at room temperature. This inspired further research worldwide. Yet the other experimental and theoretical research results didn't agree with Dillon's. Liu stated, for example, that synthesized SWCNTs can only store up to 2.4 wt% hydrogen gas at ambient temperature with a pressure of 100-120 bar (Liu et al., 1999). Even after heat treatment on SWCNTs, hydrogen uptake only increased to 4.2 wt%.

More recent research by Xu et al. (2007) states that hydrogen uptake is much lower than Dillon's and Liu's calculations. At an ambient temperature of 303 K and pressure of 100 bar, the hydrogen uptake was only 0.31-0.48 wt%. Guay et al. (2004) report hydrogen storage results in various types of carbon nanostructures using classical Monte-Carlo simulation. The findings indicate very low hydrogen uptake (below 1 wt% at 293 K) and pressures up to 10 MPa on SWCNT and multi-walled carbon nanotubes (MWCNTs) (Guay et al., 2004).

Until now, it could be said that without improvements, hydrogen storage in carbon nanostructures will not meet practical targets (Shevlin & Guo, 2008). Some theoretical and experimental studies, though, have been and are being carried out intensively to increase the storage capacity of hydrogen in CNTs through: structural optimization, controlling parameters (Zolfaghari et al., 2007), and metal doping/substitution (Reddy & Ramaprabhu, 2007). Another way to increase the adsorption capacity is to modify the CNTs to possess new characteristics or obtain completely new material. New materials receiving attention include boron carbide, boron nitride, and carbon nitride.

Cheng et al. investigated the diameter effects and chirality on hydrogen adsorption in SWCNTs using molecular dynamics simulation. Cheng focused on what diameter range and chirality for hydrogen adsorption is most energetically favorable. Cheng reported that to achieve 6.5 wt% at ambient temperatures, up to 7,500 atm pressure is needed. Pressure of up to 1,000 atm is needed on 11.8 Å diameter SWCNTs. Cheng concluded the optimum diameter for a SWCNT is about 6 Å (Liu & Cheng, 2005).

2. DISPARITY LINE UTILIZATION FACTOR

2.1. Research Flowchart

The research method for the optimization of hydrogen storage capacity will be conducted by combining results from a semi-empirical study, quantum mechanics calculations, and a theoretical approach. As shown in Figure 1, Langmuir adsorption constants (b) are one of the main factors that represent SWCNT characteristics and performance. Sticking coefficient (α) and heterogeneity parameter of adsorbent (t) can be calculated empirically. Having obtained the values of (b) and (t), adsorption energy was calculated as a function of the SWCNT diameter. Hydrogen physisorption energy was investigated using ab-initio calculations and force-matching. Through the relationship adsorption potential of SWCNTs, Langmuir constants, sticking coefficient, (α), and equilibrium pressure can theoretically be estimated as a value of monolayer coverage (θ).

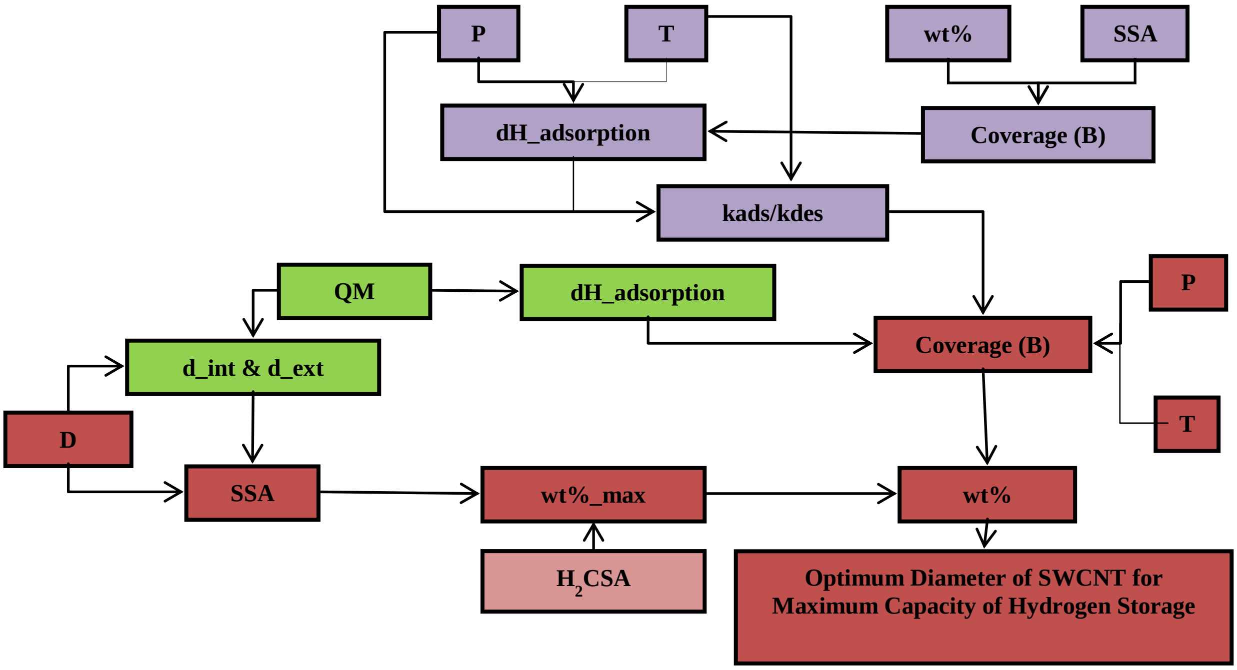

Figure 1 Research flowchart

The next step is to determine the specific occupancy area of adsorbate, SOA_{H_2}, and specific surface area (SSA) of adsorbent, SSA_{CNT}. The maximum adsorption capacity of hydrogen in various SWCNTs was calculated as a function of diameter. Adsorption capacity was analyzed at various temperatures and pressures to get the optimum SWCNT diameter. In this paper, the investigation was carried out in a pressure range of 0.1 to 10 MPa at temperatures of 233 K and 298.15 K, respectively.

2.2. First-principle Study

We calculated the interaction potential energy on hydrogen molecules and SWCNTs using ab-initio calculations performed at the MP2 method level (Møller & Plesset, 1934), def2-TZVPP basis-sets were performed with a PSI4 package (Turney et al., 2012). The SWCNT structures were simplified into a cluster model, as shown in Figure 2, to reduce computational costs. In this cluster model, the SWCNT is simplified into 24 carbon atoms. All carbon atoms located on the edge of the model are saturated with hydrogen atoms to put the system in a closed-shell configuration, which is more stable for electronic structure calculations. Several works have used similar models, stating they can provide accurate results (Mahdizadeh & Goharshadi, 2014).

In this study, we calculated single-point energy at various distances between the SWCNT wall and molecular center of hydrogen. The hydrogen molecule was placed above the center of the SWCNT's hexagonal structure (hollow site), since this is where the strongest interaction configuration between hydrogen molecule and SWCNT occurs. The illustration is shown in Figure 2. The interaction potential energy between hydrogen and SWCNT is calculated using the following equation:

$$\Delta E = E_{H_2-CNT} - \left(E_{CNT} + E_{H_2}\right) \tag{1}$$

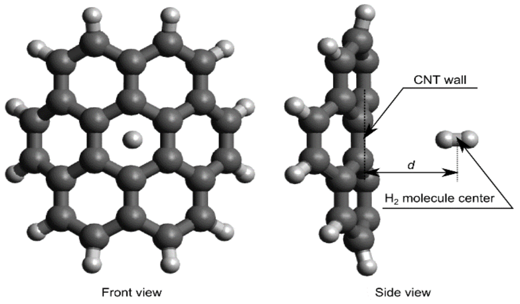

Figure 2 Cluster model of hydrogen physisorption on SWCNT (10, 0) for first-principle study

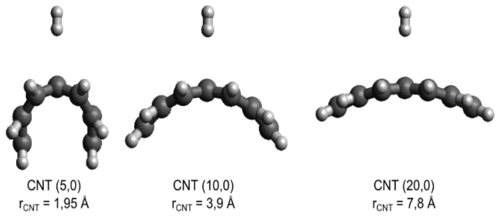

Figure 3 SWCNT with various chirality

Since the smallest SWCNT that can be synthesized is 3 Å, we chose a (5, 0) zig-zag SWCNT with a diameter of 3.9 Å. Several SWCNTs with larger chirality and diameters were also investigated to collect a sufficient amount of data for regression (see Figure 3). We considered zig-zag SWCNTs of chiral vector (5, 0), (10, 0), (20, 0), and (40, 0) respectively and a relevant diameter D of approximately 1.95, 3.9, 4.85, and 9.7 Å.

We used a force-matching method to approximate the interaction potential energy parameters on carbon and hydrogen molecules. Hydrogen molecules were modeled into isotropic or united atom models. The hydrogen atoms on the edge of SWCNT cluster models were neglected in force-matching calculations based on the assumption that it does not contribute much to the interaction potential energy (see Figure 4).

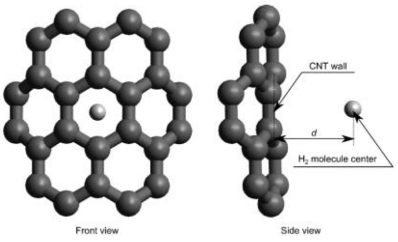

Figure 4 Isotropic model of hydrogen physisorption on SWCNT for the force-matching method to approximate potential parameters

We used the Lennard-Jones (LJ) potential function to define non-covalent interatomic potential energy between carbon and hydrogen molecules per the following equation:

$$\Delta E_{C-H_2} = 4\varepsilon\left[\left(\frac{\sigma}{r}\right)^{12} - \left(\frac{\sigma}{r}\right)^{6}\right] \tag{2}$$

3. RESULTS AND DISCUSSION

3.1. Toth Monolayer Adsorption

Based on the theory of monolayer adsorption of kinetic reaction, the Toth isothermal equation can be derived as follows (Do, 1998):

$$\theta = \frac{bP}{[1+(bP)^t]^{1/t}} \tag{3}$$

where *b* represents a Langmuir constant, *α* is the sticking coefficient, and *t* is the parameter of adsorbent surface heterogeneity characteristics. Figure 5 shows the monolayer coverage value of several SWCNT types at pressures ranging from 1 to 3.5 MPa (Takagi et al., 2007).

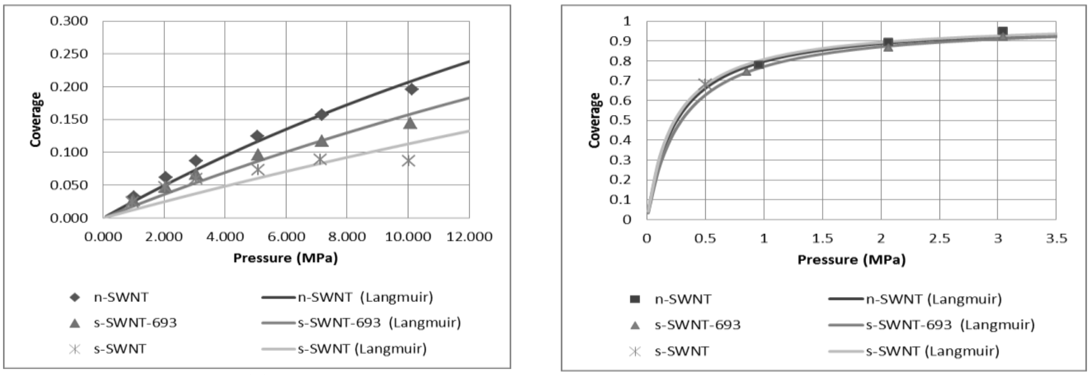

(a) (b)

Figure 5 Monolayer Coverage of varies SWCNT at temperature: (a) 303 K; and (b) 77 K

Monolayer adsorption potential energy is calculated as a function of the hydrogen molecule distance to the SWCNT walls based on Equation 1. The results of interaction potential energy calculations for (5, 0), (10, 0), (20, 0), and (40, 0) CNTs are shown in Figure 6. Figure 6 reveals that the potential energy interaction will increase as SWCNT diameters increase. This also means monolayer potential energy of SWCNT outside areas is proportional to the diameter, though not very significant.

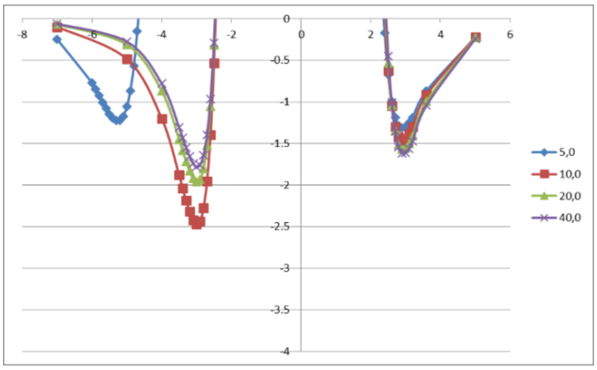

Figure 6 Ab-initio calculations and force-matching results for hydrogen physisorption on SWCNTs

The quantum mechanics method showed the adsorption energy for SWCNT external parts is between 1.35 and 1.62 kcal/mol. The lowest interaction potential energy occurred at (5, 0) SWCNT (i.e., 1.316 kcal/mol), while the highest is 1.618 kcal/mol in (40, 0) SWCNT. Han and Lee (20014) also performed calculations on the adsorption energy on the (10, 0) SWCNT using density functional theory. They obtained a value of 0.792 kcal/mol on the outside of the SWCNT. This is much smaller than our result (1.7 kcal/mol).

The left side of Figure 6 shows the reverse phenomenon; the magnitude of the monolayer potential energy value on the SWCNT interior is inversely proportional to the SWCNT interior diameter. The range of values is wider on the SWCNT exterior, which is between 1.22 and 2.43 kcal/mol. The value of the lowest interaction potential energy occurs at (40, 0) SWCNT (1.78 kcal/mol), while the greatest interaction potential energy occurs at (10, 0) SWCNT: 2,433 kcal/mol. These results are relatively similar to the investigation conducted by Srinivasu and Ghosh (2011). They reported 2.2 kcal/mol, which is slightly lower compared to the investigation using computational design reported by Jhi and Kwon (2004), around 2.86 kcal/mol.

The (5, 0) SWCNT has a different characteristic than other SWCNTs. At (5, 0) SWCNT, the adsorption energy is much higher. This shows the hydrogen molecules cannot enter the interior section. From the investigation, the σ_{C-H} value is not significantly affected by the SWCNT diameter. In general, the σ_{C-H} is 2.9 Å at interior and 3 Å at exterior. These values correspond to the those published by Jena et al. (2011), between 2.5 and 3 Å, and Gordon et al. (1999): 2.96 Å.

From the calculation on various SWCNT types, the adsorption heat (Q) is 2,317 kcal/mol and the adsorbent characteristics values are 0.56 and 0.265 at temperatures of 303 K and 77 K respectively. Empirically, we can also calculate the sticking coefficient of the adsorbent (α) for 0.101 and the value of maximum adsorption capacity wt% max of various SWCNTs. The adsorption capacity wt% and the SWCNT SSAs can be read directly from the available data.

Based on several adsorption thermodynamic parameters, the theoretical monolayer coverage on SWCNTs can be calculated. Figure 7 shows the SWCNT with a diameter of 6-7 Å has the greatest monolayer coverage, with an interior of 0.8-1 and exterior of 0.53. The amount of monolayer coverage is shrinking according to the greater diameter of SWCNT magnitude. The asymptotically increasing diameter goes towards 0.6 at the interior and 0.4 at the exterior. The relatively small monolayer coverage values are one explanation why the hydrogen adsorption at SWCNT is still a difficult target to achieve by setting the DoE at room temperature.

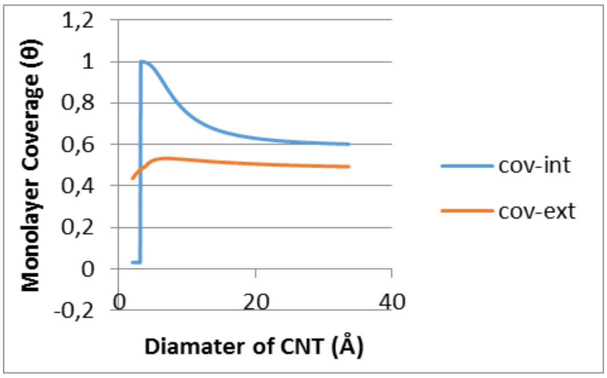

Figure 7 Monolayer coverage (θ) of treated SWCNT

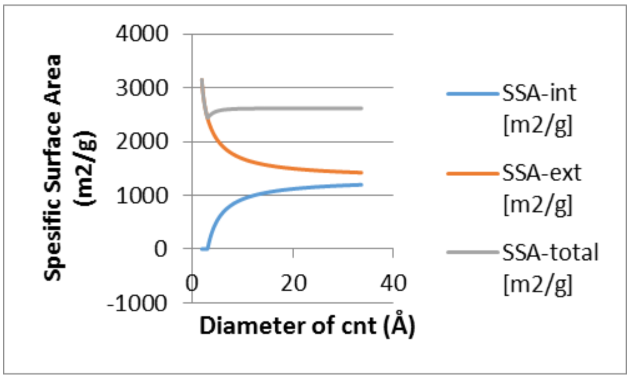

Figure 8 SSA of treated SWCNTs. The blue line shows SWCNT interior SSA. The red line shows SWCNT exterior SSA. The grey line shows total SWCNT SSA

SSA is the most important characteristic in the adsorption process involving porous solids. In this section, the SWCNT SSA value is analyzed as a function of the adsorption heat (Q). This is derived from the quantum computation and size of the monolayer coverage (θ), which is obtained by theoretical estimation.

From Figure 8, we can see that the SWCNT exterior SSA (SSA_{ext}) decreases as the SWCNT diameter increases. Meanwhile, the SWCNT interior SSA (SSA_{int}) increases as the SWCNT diameter increases. As the SWCNT has a diameter of up to 35 Å, the SSA_{int} is always smaller than the SSA_{ext}. The SSA_{ext} will asymptotically decrease towards the value of 1,400 given a greater SWCNT diameter. The SSA_{int} will asymptotically increase towards the value of 1,200.

However, the value difference between SSA_{ext} and SSA_{int} does not reveal many characteristic variances. Ultimately, the total SSA is the influential factor. The figure shows the SSA value is not affected by the size of the SWCNT diameter, which is an average 2,600 m^2/g.

3.2. Hydrogen Storage Capacity of SWCNT

The proportion of the adsorption capacity between the interior and exterior is interesting to observe. Figures 8 and 9 show that adsorption capacity is proportional to the SWCNT SSA_{ext} and SSA_{int}. At a constant pressure adsorption capacity, the interior increases along with the increasing temperature and increasing SWCNT diameter. The opposite phenomenon occurs for the exterior; the adsorption capacity increases with decreasing temperature and shrinking diameter. Ambient pressure to the adsorption capacity of the interior is always smaller than the adsorption capacity for the exterior with a temperature below 93 K and a SWCNT diameter smaller than 68 Å. A higher temperature and lower pressure are obtained proportionately to the wt% of the interior. Exterior SWCNT parts behave in the same way when the diameter decreases.

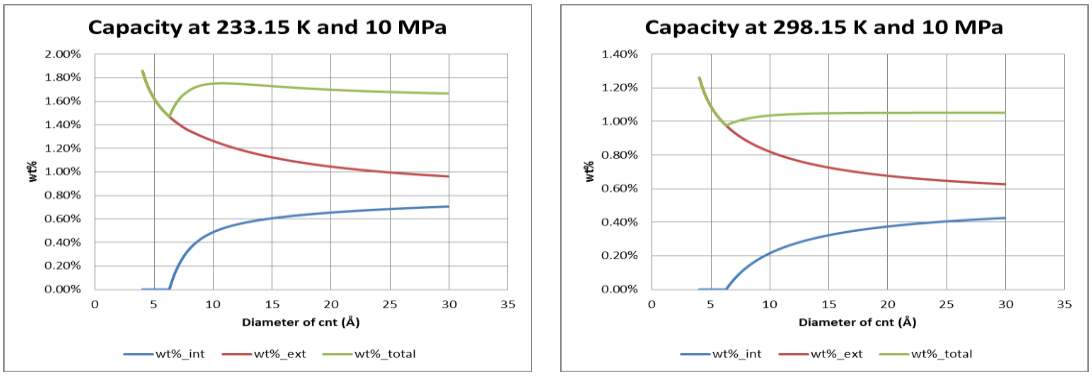

(a) (b)

Figure 9 (a) Hydrogen adsorption capacity compared to SWCNT diameter; (b) Maximum adsorption capacity at 77 K. Maximum adsorption capacity at 300 K

At room temperature and ambient pressure, there is almost no hydrogen adsorption on the SWCNT exterior. This indicates the presence of hydrogen on the SWCNT interior, not because of the adsorption energy, but due to the effects of capillarity SWCNT. With an SWCNT diameter of up to 35 Å, interior adsorption capacity is always smaller than exterior adsorption capacity.

Figure 9a shows the adsorption capacity of various SWCNT types in the pressure range of 1-10 MPa at a temperature of 233 K and 298.15 K. Figure 9b reveals that the influence on the adsorption capacity diameter gets smaller with a lower temperature and higher pressure. At temperatures of 233 K and a pressure of 10 MPa, a maximum adsorption capacity of 1.75 wt% was recorded on the SWCNT's 8-12 Å diameter. This result is close to the research study conducted by Cheng et al., that the maximum adsorption capacity was achieved at a diameter of about 6 Å (Cheng et al., 2005). With this diameter, higher pressures of up to 10 MPa can be obtained if the maximum adsorption capacity does not exceed 2 wt%. At room temperature, with any SWCNT diameter, and under moderate pressure, the maximum adsorption capacity is relatively small: only 0.02 wt% and 1.1 wt% at a pressure of 10 MPa.

4. CONCLUSION

With combined semi-empirical research, a theoretical approach, and force-matching methodology, the average SWCNT SSA value can be estimated (i.e., 2,600 m^2/g). The SSA values do not correlated with the SWCNT diameter. With a range of temperature and pressure variations, an optimum SWCNT diameter of 8-12 Å was obtained. A maximum adsorption capacity of 1.75 wt% at temperatures of 233 K and a pressure of 10 MPa was estimated at the diameter. At room temperature and under a pressure of 10 MPa, the maximum adsorption capacity was 1.1 wt%. These results still do not meet the target set by the DoE, so an investigation is necessary to modify the structure or add elements to the SWCNT. This will hopefully improve the outcome.

5. ACKNOWLEDGMENT

We gratefully acknowledge the support of this research by the Directorate General of Higher Education, Ministry of Education, and Culture of the Republic of Indonesia through their research funding program: Hibah Bantuan Desertasi Program Doktor 2014.

6. REFERENCES

Barghi, S.H., Tsotsis, T.T., Sahimi, M., 2014. Chemisorption, Physisorption and Hysteresis During Hydrogen Storage in Carbon Nanotubes. *International Journal of Hydrogen Energy,* Volume 39(3), pp. 1390–1397

Biniwale, R.B., Rayalu, S., Devotta, S., Ichikawa, M., 2008. Chemical Hydrides: A Solution to High Capacity Hydrogen Storage and Supply. *International Journal of Hydrogen Energy,* Volume 33(1), pp. 360–365

Chen, C.-h., Huang, C.-c., 2008. Enhancement of Hydrogen Spillover onto Carbon Nanotubes with Defect Feature. *Microporous and Mesoporous Materials,* Volume 109(1-3), pp. 549–559

Cheng, H., Cooper, A.C., Pez, G.P., Kostov, M.K., Piotrowski, P., Stuart, S.J., 2005. Molecular Dynamics Simulations on the Effects of Diameter and Chirality on Hydrogen Adsorption in Single Walled Carbon Nanotubes. *The Journal of Physical Chemistry B,* Volume 109(9), pp. 3780–3786

Dillion, A.C., Jones, K.M., Bekkedahl, T.A., Kiang, C.H., Bethune, D.S. Heben, M.J., 1997. Storage of Hydrogen in Single-walled Carbon Nanotubes. *Nature*, Volume 386, pp. 377–379

Do, D.D., 1998. *Adsorption Analysis: Equilibria and Kinetics* (Chemical Engineer Series, Volume 2). Imperial College Press

Gayathri, V., Devi, N.R., Geetha, R., 2010. Hydrogen Storage in Coiled Carbon Nanotubes. *International Journal of Hydrogen Energy,* Volume 35(3), pp. 1313–1320

Guay, P., Stansfield, B.L., Rochefort, A., 2004. On the Control of Carbon Nanostructures for Hydrogen Storage Applications. *Carbon*, Volume 42(11), pp. 2187–2193

Gordon, P.A., Saeger, R.B., 1999. Molecular Modeling of Adsorptive Energy Storage: Hydrogen Storage in Single-walled Carbon Nanotubes. *Industrial & Engineering Chemistry Research*, Volume 38(12), pp. 4647–4655

Hamilton, C.W., Baker, R.T., Staubitz, A., Manners, I., 2009. B–N Compounds for Chemical Hydrogen Storage. *Chemical Society Reviews*, Volume 38(1), pp. 279–293

Han, S.S., Lee, H.M., 2004. Adsorption Properties of Hydrogen on (10, 0) Single-walled

Carbon Nanotube through Density Functional Theory. *Carbon,* Volume 42(11), pp. 2169–2177

Jena, P., 2011. Materials for Hydrogen Storage: Past, Present, and Future. *J. Phys. Chem. Lett,* Volume 2(3), 206–211

Jhi, S.-h., Kwon, Y.-k., 2004. Hydrogen Adsorption on Boron Nitride Nanotubes: A Path to Room-temperature Hydrogen Storage. *Physical Review B,* Volume 69-245407(24), pp. 1–5

Knippenberg, M.T., Stuart, S.J., Cheng, H., 2008. Molecular Dynamics Simulations on Hydrogen Adsorption in Finite Single Walled Carbon Nanotube Bundles. *Journal of Molecular Modeling,* Volume 14(5), pp. 343–351

Liu, C., Cheng, H.-m., 2005. Carbon Nanotubes for Clean Energy Applications. *Journal of Physics D: Applied Physics,* Volume 38(14), R231

Liu, C., Fan, Y., Liu, M., Cong, H.T., Cheng, H.M., Dresselhaus, M.S., 1999. Hydrogen Storage in Single-walled Carbon Nanotubes at Room Temperature. *Science,* Volume 286(5442), pp. 1127–1129

Luo, Y., Wang, P., Ma, L.-p., Cheng, H.-m., 2007. Enhanced Hydrogen Storage Properties of MgH_2 Co-catalyzed with NbF_5 and Single-walled Carbon Nanotubes. *Scripta Materialia,* Volume 56(9), pp. 765–768

Mahdizadeh, S.J., Goharshadi, E.K., 2014. Hydrogen Storage on Silicon, Carbon, and Silicon Carbide Nanotubes: A Combined Quantum Mechanics and Grand Canonical Monte Carlo Simulation Study. *International Journal of Hydrogen Energy,* Volume 39(4), pp. 1719–1731

Møller, C., Plesset, M.S., 1934. Note on an Approximation Treatment for Many-electron Systems. *Physical Review,* Volume 46(7), pp. 618–622

Qiu, N.-x., Tian, Z.-y., Guo, Y., Zhang, C.-h., Luo, Y.-p., Xue, Y., 2014. A First-principle Study of Calcium-decorated BC_2N Sheet Doped by Boron or Carbon for High Hydrogen Storage. *International Journal of Hydrogen Energy,* Volume 39(17), pp. 9307–9320

Reddy, A.L.M., Ramaprabhu, S., 2007. Hydrogen Storage Properties of Nanocrystalline Pt Dispersed Multi-walled Carbon Nanotubes. *International Journal of Hydrogen Energy,* Volume 32(16), pp. 3998–4004

Sankaran, M., Viswanathan, B., 2007. Hydrogen Storage in Boron Substituted Carbon Nanotubes. *Carbon,* Volume 45(8), pp. 1628–1635

Satyapal, S., Petrovic, J., Read, C., Thomas, G., Ordaz, G., 2007. The US Department of Energy's National Hydrogen Storage Project: Progress Towards Meeting Hydrogen-Powered Vehicle Requirements. *Catalysis Today,* Volume 120(3), pp. 246–256

Shevlin, S.A., Guo, Z.X., 2008. High-capacity Room-temperature Hydrogen Storage in Carbon Nanotubes via Defect-modulated Titanium Doping. *The Journal of Physical Chemistry C,* Volume 112(44), pp. 17456–17464

Srinivasu, K., Ghosh, S.K., 2011. Theoretical Studies on Hydrogen Adsorption Properties of Lithium Decorated Diborene ($B_2H_4Li_2$) and Diboryne ($B_2H_2Li_2$). *International Journal of Hydrogen Energy,* Volume 36(24), pp. 15681–15688

Takagi, H., Soneda, Y., Hatori, H., Zhu, Z.H., Lu, M., 2007. Effects of Nitric Acid and Heat Treatment on Hydrogen Adsorption of Single-walled Carbon Nanotubes. *Australian Journal of Chemistry,* Volume 60(7), pp. 519–523

Turney, J.M., Simmonett, A.C., Parrish, R.M., Hohenstein, E.G., Evangelista, F.A., Fermann, J.T., Mintz, B.J., Burns, L.A., Wilke, J.J., Abrams, M.L., Russ, N.J., Leininger, M.L., Janssen, C.L., Seidl, E.T., Allen, W.D., Schaefer, H.F., King, R.A., Vallev, E., Sherrill, C. D., Crawford, T.D., Wiley, J., Sons, 2012. Psi4: an Open-Source Ab Initio Electronic Structure Program. *Computational Molecular Science,* Volume 2(4), pp. 556–565

Xu, W.-C., Takahashi, K., Matsuo, Y., Hattori, Y., Kumagai, M., Ishiyama, S., Kaneko, K., Iijima, S., 2007. Investigation of Hydrogen Storage Capacity of Various Carbon Materials.

International Journal of Hydrogen Energy, Volume 32(13), pp. 2504–2512

Zheng, J., Liu, X., Xu, P., Liu, P., Zhao, Y., Yang, J., 2012. Development of High Pressure Gaseous Hydrogen Storage Technologies. *International Journal of Hydrogen Energy,* Volume 37(1), pp. 1048–1057

Zhou, L., 2005. Progress and Problems in Hydrogen Storage Methods. *Renewable and Sustainable Energy Reviews,* Volume 9(4), pp. 395–408

Zolfaghari, A., Hashemi, F., Pourhossein, P., Jooya, H. Z., 2007. Molecular Dynamics Simulations on the Effect of Temperature and Loading in H_2 Exohedral Adsorption on (3, 3) and (9, 9) SWCNTs. *International Journal of Hydrogen Energy,* Volume 32(18), pp. 4889–4893